Polarity independent high thermal stability of interstitial Mn in GaAs

L. M. C. Pereira,[1,2,3,*] U. Wahl,[3,4] S. Decoster,[1] J. G. Correia,[3,4]
L. M. Amorim,[1] M. R. da Silva,[4] J. P. Araújo,[2] and A. Vantomme[1]

[1] *Instituut voor Kern- en Stralingsfysica and INPAC, K.U.Leuven, 3001 Leuven, Belgium*
[2] *IFIMUP and IN-Institute of Nanoscience and Nanotechnology, DFA-FCUP, 4169-007 Porto, Portugal*
[3] *Instituto Tecnológico e Nuclear, UFA, 2686-953 Sacavém, Portugal*
[4] *Centro de Física Nuclear da Universidade de Lisboa, 1649-003 Lisboa, Portugal*

(Dated: August 4, 2011)

We report on the lattice location of Mn impurities (< 0.05%) in undoped (semi-insulating) and heavily *n*-type doped GaAs, by means of β^- emission channeling from the decay of ^{56}Mn produced at ISOLDE/CERN. In addition to the majority substituting for Ga, we locate up to 30% of the Mn impurites on tetrahedral interstitial sites with As nearest neighbors. In line with the recently reported high thermal stability of interstitial Mn in heavily *p*-type doped GaAs [L. M. C. Pereira *et al.*, Appl. Phys. Lett. **98**, 201905 (2011)], the interstitial fraction is found to be stable up to 400°C, with an activation energy for diffusion of 1.7–2.3 eV. By varying the concentration of potentialy trapping defects, without a measurable effect on the migration energy of the interstitial impurities, we conclude that the obsereved high thermal stability is characteristic of isolated intersititial Mn. Being difficult to reconcile with the general belief that interstitial Mn is the donor defect that out-diffuses at ∼200°C, these findings motivate a carefull reassessment of the stuctural effects of low temperature annealing of $Ga_{1-x}Mn_xAs$, with potential implications on the prospects for achieving higher Curie temperatures.

PACS numbers: 75.50.Pp, 61.72.uj, 61.72.Cc

I. INTRODUCTION

One of the most well understood dilute magnetic semiconductors (DMS), $Ga_{1-x}Mn_xAs$ has become an exceptional material in which to study the physics of carrier-mediated ferromagnetism in semiconductors[1–3] and for the development of proof-of-concept semiconductor-based spintronic devices.[4] Based on this sound understanding of $Ga_{1-x}Mn_xAs$, both fundamental and applied, the increase in Curie temperature (T_C) above the current record value of 190 K to above room temperature remains a major goal in the DMS field.[5]

It has been theoretically and experimentally established that the T_C of $Ga_{1-x}Mn_xAs$ increases with increasing Mn concentration and hole concentration p.[6] More precisely, T_C increases with effective Mn concentration, which takes into account the balance between the fractions of Mn substituting for Ga (Mn_{Ga}) and on interstitial sites (Mn_I). While Mn_{Ga} provides both the localized magnetic moment and the itinerant hole that mediates the magnetic coupling, Mn_I has a two-fold compensating effect: magnetic, as Mn_I-Mn_{Ga} pairs couple antiferromagnetically, and electrical, since double donor Mn_I compensates Mn_{Ga} acceptors. As a consequence of this self-compensation, while the amount of Mn that can be incorporated in high quality metallic $Ga_{1-x}Mn_xAs$ has been remarkably increased throughout the years up to $x \approx 0.10$, p and T_C persistently fail to follow.[6,7] Thermal annealing near the growth temperature (∼200°C) increases p and consequently T_C, but a significant fraction of the initially introduced Mn atoms remains inactive.[6,8] This partial activation by annealing (∼200°C) was attributed to the out-diffusion of a compensating defect with low thermal stability,[8] with an activation energy (E_a) of 0.7 eV,[9] which has been identified as interstitial Mn.[9,10] This established the belief that pure substitutional Mn doping can be achieved by low-temperature (∼200°C) thermal annealing. Since then, attempts to increase T_C above room temperature have focused on increasing the Mn concentration that can be incorporated in $Ga_{1-x}Mn_xAs$. However, film growth development beyond $x \approx 0.10$ and (and thus of $T_C \approx 190$ K) faces significant technical challenges.[6,11]

Recently, we reported on the lattice location of Mn in heavily *p*-type doped GaAs.[12] We identified the lattice site occupied by interstitial Mn as the tetrahedral interstitial site with As nearest neighbors (T_{As}) and, more importantly, gave evidence of its high thermal stability, up to 400°C, with an effective activation energy (E_a) for diffusion of 1.7–2.3 eV. Being difficult to reconcile with the general belief that Mn_I is the donor defect that out-diffuses at ∼200°C with $E_a = 0.7$ eV, these results raise two important questions:

1. What is the origin of such a high activation energy? Is it a characteristic of interstitial Mn in T_{As} sites or is it due to trapping by oppositely charged acceptor defects (i.e. substitutional Mn in $Ga_{1-x}Mn_xAs$ or Zn acceptors in our previous study in heavily *p*-type doped GaAs)? While the migration barrier for an isolated Mn_I atom was estimated by *ab initio* calculations to be only 0.8 eV,[9] pairing with Mn_{Ga} acceptors was estimated to add up to 0.8 eV of dissociation energy,[13] which could explain the high effective migration energy.

2. What are the implications of such a high ther-

mal stability of interstitial Mn on the strategies and prospects to achieve higher Curie temperatures in $Ga_{1-x}Mn_xAs$? If interstitial Mn is immobile in GaAs up to 400°C (Ref. 12), while Mn clustering is known to set in already at 282°C in $Ga_{1-x}Mn_xAs$ (Ref. 10), can pure substitutional doping be achieved in $Ga_{1-x}Mn_xAs$ by thermal annealing?

We address these questions here by studying, as a function of annealing temperature, the lattice location of Mn in both semi-insulating (SI) and highly *n*-type doped (n^+) GaAs using β^- emission channeling. Comparing these to our previous results on highly *p*-type doped (p^+) GaAs,[12] we investigate if the higher thermal stability of interstitial Mn can be ascribed to trapping by electrical defects (question 1). Comparing the thermal stabilities of Mn in interstitial and substitutional sites in GaAs to the temperature regime where Mn aggregation and phase segregation is known to occur in $Ga_{1-x}Mn_xAs$, we discuss if, above its mobility threshold, interstitial Mn atoms are more likely to out-diffuse or aggregate with other Mn atoms (question 2).

II. EXPERIMENT

A. Emission channeling technique

The emission channeling (EC) technique is designed to determine the lattice location of impurities in single crystals, making use of the charged particles emitted by a radioactive isotope of the impurity element under study.[14] The screened Coulomb potential of atomic rows and planes determines the anisotropic scattering of the particles emitted isotropically during decay. Along low-index crystal directions of single crystals, this anisotropic scattering results is well defined channeling or blocking effects. Because these effects strongly depend on the initial position of the emitted particles, they lead to emission patterns which are characteristic of the lattice site(s) occupied by the probe atoms. Angular-dependent emission patterns are recorded along various crystallographic axis using a position- and energy-sensitive detection system similar to that described in Ref. 15. The theoretical emission patterns for probes occupying possible lattice sites are calculated using the *manybeam* formalism for electron channeling in single crystals.[14] Quantitative lattice location is provided by fitting the experimental patterns with theoretical ones using the two-dimensional fit procedure outlined in Ref. 15. Corrections for secondary electrons that reach the detector were implemented by subtracting an isotropic background from every pattern. This secondary electron contribution is estimated based on Geant4[16,17] simulations of electron scattering, taking into account the elemental composition and geometry of the sample, sample holder and vacuum chamber. Several reviews on emission channeling can be found in the literature.[14,18–20]

The technique offers a number of advantages when compared to other lattice location techniques. Because EC relies on 2-dimensional emission patterns (measured using position sensitive detectors) which are directly compared to numerical simulations, it provides unambiguous and quantitative lattice location superior to conventional ion-channeling techniques. In addition, it is extremely sensitive in the sense that it requires a small number of impurities, down to 10^{10} atoms, which makes it particularly suited to study very dilute systems, unlike synchrotron based techniques such as X-ray absorption fine structure (XAFS), which require a number of impurities several orders of magnitude above. Probably one of the strongest features of the EC technique is its applicability to those cases where significant fractions of the impurities occupy more than one lattice site. This multisite lattice location capability of EC has allowed us, for example, to establish the amphoteric (both Ga- and N-substitutional) nature of As in GaN[21] and to identify, in addition to the majority fractions in cation sites, significant fractions of Co and Mn impurities in the anion (O) site in ZnO[22] and of Mn impurities in the anion (N) site of GaN.[23] Although in principle such minority versus majority occupancies can also be quantified using XAFS, unambiguous identification of minority sites is extremely challenging, because the technique relies on complex multiparameter fitting of the spectra using calculated model structures. For the case of Mn impurities in GaAs in particular, these limitations of XAFS and conventional ion-channeling techniques in identifying minority sites has resulted in either (i) an incomplete identification of the Mn interstitial site or (ii) a complete identification that conflicts with the theoretical prediction: (i) Based on ion channeling[10] and XAFS[24] experiments, the Mn impurities were found to occupy Ga substitutional sites (majority) and tetrahedral interstitial (T) sites (minority), without however being possible to identify which of the two possible T sites, i.e. with Ga (T_{Ga}) or As (T_{As}) nearest neighbors; (ii) Based on XAFS experiments the interstitial site was identified as the S_{Ga}, which is in disagreement with *ab initio* calculations estimating an energy 0.35 eV lower for Mn in T_{As} sites compared to T_{Ga}.[9] This inconsistency among XAFS reports and disagreement with our previous emission channeling results[12] can be explained by the limitations of XAFS in distinguishing the chemical nature of neighbors with similar atomic numbers, as is the case of Ga and As. With emission channeling, the distinction between T_{Ga} and T_{As} is a direct structural effect, as we describe next.

Examples for possible lattice sites of high symmetry in the GaAs zincblende structure are shown in Fig. 1. In addition to the substitutional Ga (S_{Ga}) and As (S_{As}) sites and the tetrahedral interstitial sites with Ga (T_{Ga}) and As (T_{As}) nearest neighbors, the following interstitial sites are shown: interstitial sites along the ⟨111⟩ direction, i.e. the bond center (BC), antibonding Ga (AB_{Ga}), antibonding As (AB_{As}) and the hexagonal site (H); interstitial sites along the ⟨100⟩ direction, in either the Ga or

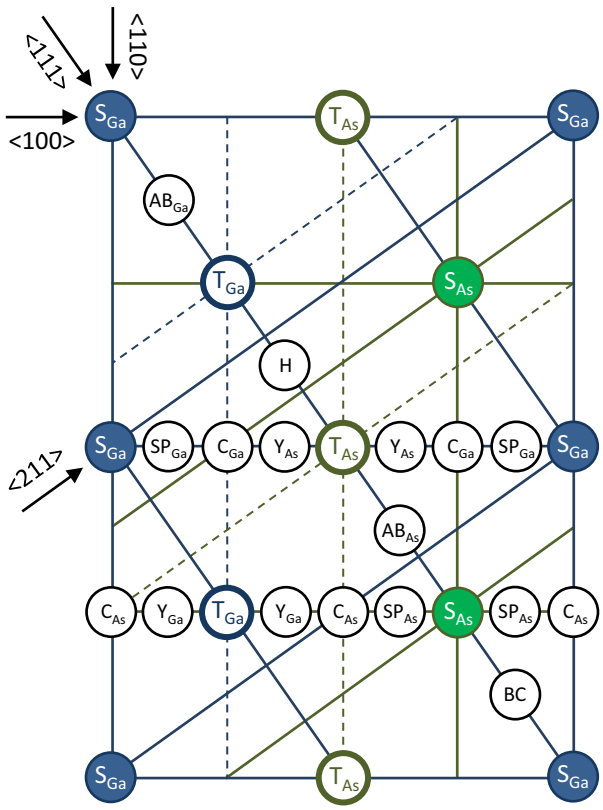

FIG. 1: (Color online) The {110} planes in the GaAs zincblende lattice, showing the following sites: the substitutional Ga (S_{Ga}) and As (S_{As}) sites; the tetrahedral interstitial sites with Ga (T_{Ga}) and As (T_{As}) nearest neighbors; interstitial sites along the ⟨111⟩ direction, i.e. the bond center (BC), antibonding Ga (AB_{Ga}), antibonding As (AB_{As}) and the hexagonal site (H); interstitial sites along the ⟨100⟩ direction, in either the Ga or the As rows, i.e. the split interstitials (SP_{Ga} and SP_{As}), the "C" sites with C_{2v} symmetry (C_{Ga} and C_{As}) and the "Y" sites (Y_{Ga} and Y_{As}). Along the ⟨100⟩, ⟨111⟩, ⟨110⟩ and ⟨211⟩ directions, the rows of Ga and As atoms are indicated (lines), as well as the rows of the T_{Ga}) and As (T_{As} sites (dashed lines). Note that, along the ⟨111⟩ direction, the substitutional (S_{Ga} and S_{As}) and tetrahedral interstitial (T_{Ga} and T_{As}) sites are all located on the same row; along the ⟨100⟩ direction, S_{Ga} is on the same row as T_{As}, and S_{As} is on the same row as T_{Ga}.

the As rows, i.e. the split interstitials (SP_{Ga} and SP_{As}), the "C" sites with C_{2v} symmetry (C_{Ga} and C_{As}) and the "Y" sites (Y_{Ga} and Y_{As}). Figure 2 shows the theoretical emission patterns along the ⟨100⟩, ⟨111⟩, ⟨110⟩ and ⟨211⟩ axes for 100% of ^{56}Mn atoms on substitutional sites (S_{Ga} and S_{As}) and tetrahedral interstitial sites (T_{Ga} and T_{As}). Because S_{Ga}, S_{As}, T_{Ga} and T_{As} sites are located on the same row along the ⟨111⟩ axis (1), they are all equivalent in the lattice projection onto the plane perpendicular to the ⟨111⟩ direction and, consequently, the corresponding ⟨111⟩ emission patterns are undestinguishable (Fig. 2, second row). Similarly, along the ⟨100⟩ direction, because S_{Ga} is on the same row as T_{As}, and S_{As} is on the same row as T_{Ga}, the corresponding ⟨100⟩ emission patterns are undestinguishable within these two pairs of sites. In order to unambiguously distinguish these sites it is thus necessary to measure also along the ⟨110⟩ and ⟨211⟩ directions, which separate the corresponding rows (see the dashed lines in Fig. 1). This results in emission patterns with distinct anisotropies (Fig. 2, third and fourth rows) and thus allows for the unambiguous indentification of the occupied lattice sites. In particular, due to the mirror-asymmetry of the ⟨110⟩ and ⟨211⟩ directions, the two T sites are unambiguoulsy distinguished (patterns inside the gray square in Fig. 2).

B. Experimental details

Radioactive ^{56}Mn ($t_{1/2} = 2.56$ h) was implanted at the on-line isotope separator facility ISOLDE at CERN, which provides mass-separated beams of radioactive Mn isotopes produced by means of 1.4-GeV proton-induced nuclear fission from uranium carbide UC_2 targets and chemically selective laser ion sources.[25] The samples consisted of ⟨100⟩ GaAs single crystals, undoped semi-insulating (s.i.) and heavily n-type doped (n^+). Material properties and implantation details are summarized in Table I, where we also include our previous experiments on heavily p-type doped (p^+) GaAs.[12] All implantations were performed at room temperature under a tilt angle of 17°. Angular-dependent emission yields of the β^- particles emitted during decay to stable ^{56}Fe were measured at room temperature, along four crystallographic directions, ⟨100⟩, ⟨111⟩, ⟨110⟩ and ⟨211⟩, in the as-implanted state and after *in situ* capless annealing under vacuum ($< 10^{-5}$ mbar) in steps of 50°C (10 min) up to 700°C. These patterns were recorded using a position- and energy-sensitive detection system similar to that described in Ref. 15. Given the relatively short half-life of ^{56}Mn ($t_{1/2} = 2.56$ h), this system was installed on-line and upgraded with self-triggering readout chips for the Si pad detectors, enabling measurements during and/or immediately after implantation with count rates of up to several kHz.

Theoretical patterns were calculated for probes occupying substitutional Ga (S_{Ga}) and As (S_{As}) sites with varying root-mean-square (rms) displacements, the high symmetry interstitial sites described above and interstitial sites resulting from displacements along the ⟨100⟩ and ⟨111⟩ directions. The GaAs crystallographic parameters and room temperature atomic displacements used in the *manybeam* simulations can be found in Ref. 26.

III. RESULTS AND DISCUSSION

Next we present and discuss the results in two parts. First we determine the lattice sites occupied by Mn in GaAs, in particular with respect to T_{As} versus T_{Ga} in-

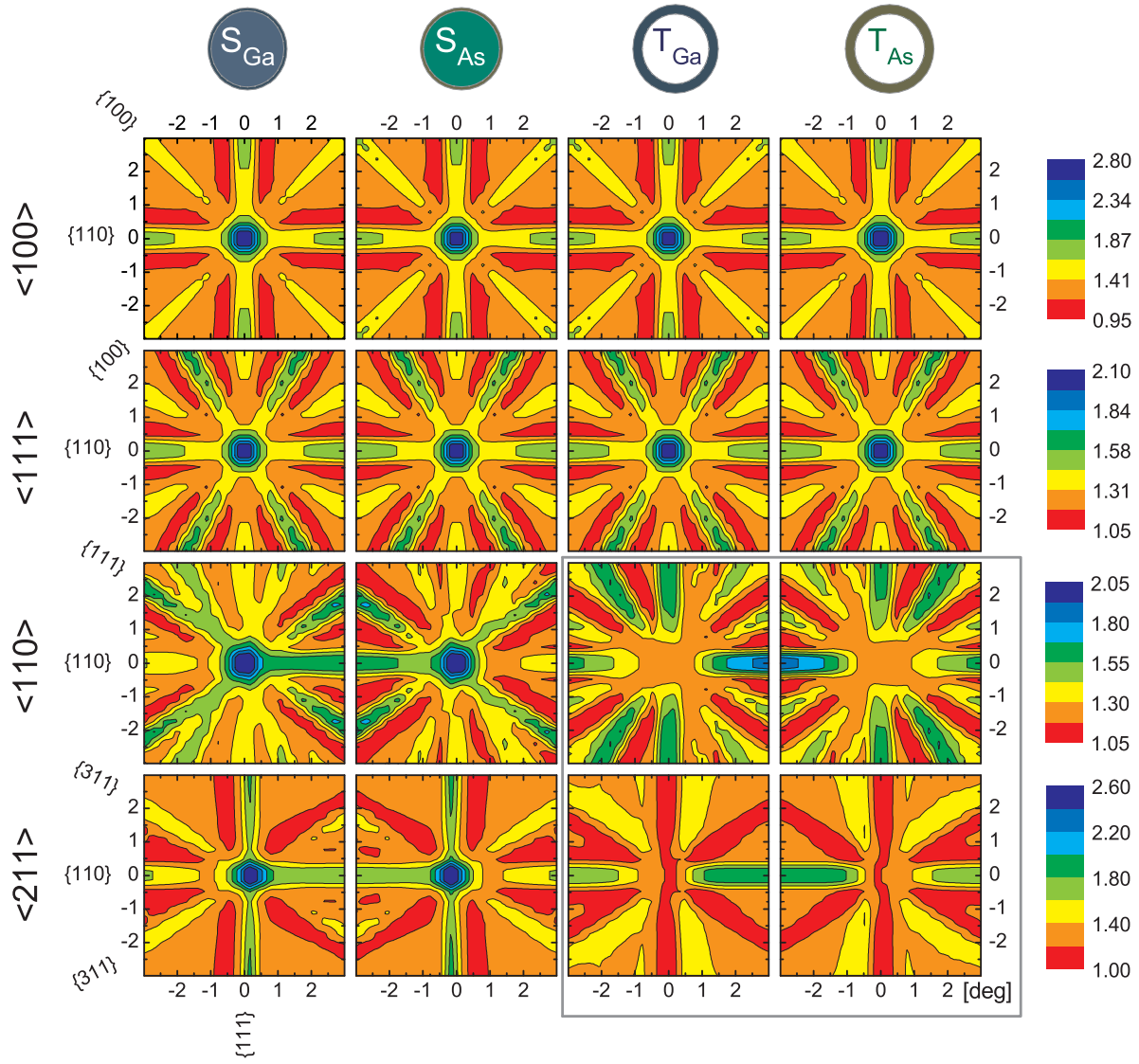

FIG. 2: (Color online) Simulated channeling patterns for 100% of emitter atoms (^{56}Mn) on substitutional Ga (S_{Ga}) and As (S_{As}) sites, and tetrahedral interstitial sites with Ga (T_{Ga}) and As (T_{As}) nearest neighbors, along the $\langle 100\rangle$, $\langle 111\rangle$, $\langle 110\rangle$ and $\langle 211\rangle$ directions.

terstitial sites, and compare it to the results of previous studies using XAFS and ion-channeling techniques. We then analyze the changes observed upon annealing in terms of thermal stability and diffusion.

A. Lattice location: substitutional and interstitial T sites

For both n^+ and semi-insulating GaAs, for all four measured directions, the calculated S_{Ga} patterns gave by far the best agreement, showing that the majority of the probe atoms occupy Ga sites, as expected. The fitting routine was then allowed to include, in addition to S_{Ga}, a second lattice site, for which all the simulated sites were tested. The S_{Ga} + T_{As} double occupancy gives the best fit compared to all other combinations and considerably improves the S_{Ga} single-site fit. As an example for the good match between experiment and simulated patterns, Fig. 3 compares the normalized experimental β^- emission yields along the four directions ((a)-(d)) of the semi-insulating (s.i.) sample measured following 100°C annealing with the best fits of theoretical patterns ((e)-(h)). These fits correspond to a mixed occupancy of 70% on substitutional Ga sites (S_{Ga}) and 30% in tetrahedral interstitial sites with As nearest neighbors (T_{As}). Introducing a third site yields only insignificant fit improvements. Possible fractions on other sites are estimated to be below 5%, which is considered the technique sensitivity. In particular for T_{As} versus versus T_{Ga} sites,

polarity	dopant	resistivity [Ωcm]	carrier concentration [cm^{-3}]	^{56}Mn fluence [at. cm^{-2}]	implantation energy [keV]	projected ion range (R_p) [Å]	projected ion straggling [Å]	peak ^{56}Mn concentration [at. cm^{-3}]
n^+	Te	0.6 – 2×10^{-3}	1.1 – 5×10^{18}(e^-)	2 × 10^{13}	40	???	???	5.4×10^{18}
s.i.	–	1.4×10^{8}	–	2 × 10^{13}	30	???	???	6.7×10^{18}
p^+	Zn	0.6 – 2×10^{-3}	1.4 – 6×10^{19}(h^+)	2 × 10^{13}	50	313	168	4.6×10^{18}

TABLE I: Sample and implantation details. All implantations were performed at room temperature under a tilt angle of 17°. The ^{56}Mn peak concentration and the projected ion range (R_p) and straggling were estimated using MARLOWE code [M. T. Robinson, Phys. Rev. B **40**, 10717 (1989)]. The details of our previous work on p^+ GaAs [L. M. C. Pereira *et al.*, Appl. Phys. Lett. **98**, 201905 (2011)] are also included.

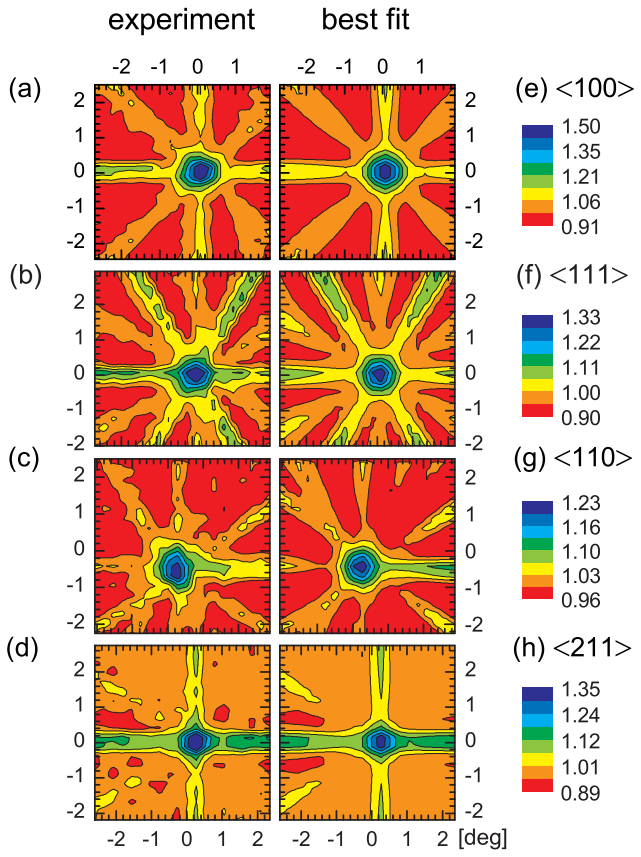

FIG. 3: (color online) (a)-(d) Normalized experimental β^- emission channeling patterns (s.i. GaAs) in the vicinity of the ⟨100⟩, ⟨111⟩, ⟨110⟩ and ⟨211⟩ directions following annealing at 100°C. (e)-(h) Corresponding best fits yielding 70% and 30% of the Mn atoms on S_{Ga} and T_{As} sites respectively.

the fitted T_{Ga} fraction is always below 5% when the routine is allowed to include S_{Ga}, T_{As} and T_{Ga} sites. This identification of the T_{As} site over T_{Ga} is consistent with our previous results on p^+ GaAs[12] and *ab initio* calculations yielding an energy 0.35 eV lower for Mn in T_{As} sites compared to T_{Ga}.[9] It is indeed natural that, due to the Coulomb interaction, positively charged Mn_I^{2+} defects have a lower energy when coordinated by negatively charged As anions rather than by positively charged Ga cations. It is thus quite surprising that previous XAFS experiments resulted in the identification of S_{Ga} + T_{Ga} occupancy,[27,28] which most likely results from the limitations of XAFS when it comes to distinguishing the chemical nature of neighbors with similar atomic numbers, as is the case of Ga and As. With emission channeling, the distinction between T_{Ga} and T_{As} sites is a direct structural effect related to the mirror-asymmetry of the ⟨110⟩ and ⟨211⟩ directions of the GaAs lattice, as described above.

We must note however that the T_{As} site may be energetically favorable over T_{Ga} only for *isolated* Mn_I defects. For very high Mn concentrations (few %), the probablility of formation of substitutional-interstitial (Mn_{Ga}–Mn_I) pairs or even larger complexes is not negligeble. In such complexes, the Coulomb attraction between opositely charged Mn_{Ga} acceptors and Mn_I donors may conteract the repulsion between positively charged Mn_I and Ga cations: since the distance between neighboring S_{Ga} and T_{Ga} sites (2.45 Å) is smaller than that between neighboring S_{Ga} and T_{As} sites (2.83 Å), the decrease in Coulomb energy by decreasing the Mn_{Ga}–Mn_I distance may counterbalence the increase in Coulomb energy by changing the Mn_I coordination to Ga cations. Indeed, *ab initio* calculations have predicted that the energy of a Mn_I atom in one of the four T_{Ga} sites neighboring a Mn_{Ga} defect is the same as in one the six T_{As}.[9] Moreover, it was also predicted that the energy barrier between the two sites is small enough to allow for Mn_I atoms to swap between the two types of sites even at room temperature.[9] Therefore, one can not exclude that, for very high concentrations of Mn and when Mn_{Ga}–Mn_I pairs *do* form, part of the interstitial fraction occupies T_{Ga} sites.

B. Thermal stability and diffusion

The Ga-substitutional and T_{As} interstitial fractions are shown in Fig. 4, as a function of annealing temperature, for both n^+ and semi-insulating GaAs. The results of our previous experiments on p^+ GaAs are also included.[12] The behavior is strikingly similar for all three

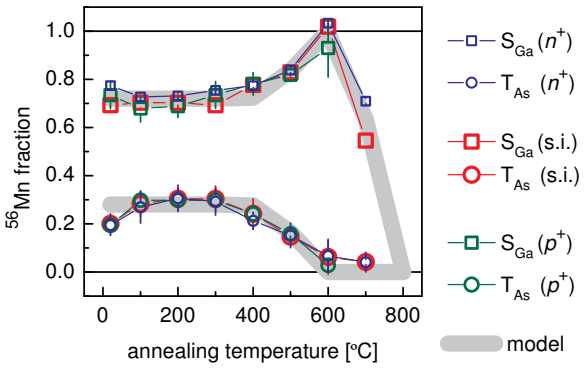

FIG. 4: (color online) Fractions of ^{56}Mn in S_{Ga} (□) and T_{As} (○) sites in n^+, semi-insulating and p^+ GaAs, derived from the fits to the experimental patterns. The data for p^+ GaAs is from [L. M. C. Pereira *et al.*, Appl. Phys. Lett. **98**, 201905 (2011)]. The gray line is given by the model of vacancy-limited diffusion of interstitial and substitutional Mn, described in the text.

materials and can be divided in three regimes:

$T \leq 300°$**C:** About 70% of the implanted Mn substitutes for Ga while the remaining 30% occupies T_{As} sites. Within the experimental error, the total $S_{Ga} + T_{As}$ fraction is 100%, which confirms that fractions on other sites are indeed negligeble. The kink at 100°, although within experimental error, is quite reproducible in the three experiments, which indicates that it is not mere experimental scatering. An increase in interstitial Mn on the expense of the substitutional fraction to the can in principle be explained as follows. If the Ga interstitials created during implantation become mobile at temperatures $\leq 100°$C, during the annealing at 100°C they can migrate and either recombine with Ga vacancies or replace substitutional Mn atoms via a kick-out mechanism ($Mn_{Ga} + Ga_I \rightarrow Mn_I + Ga_{Ga}$). The latter mechanism can thus explain the increase of the interstitial fraction on the expense of substitutional Mn. Note that, due to the Coulomb attraction between (most likely) opositly charged Ga interstitials (donors) and substitutional Mn (acceptors), this kick-out mechanism can be quite efficient even in the very dilute regime of our samples.

$400°\text{C} \leq T \leq 600°$**C:** The substitutional fraction increases on the expense of the interstitial fraction. At 600°C the interstitial fraction has almost completely converted into substitutional. The fact that the total $S_{Ga} + T_{As}$ fraction remains constant indicates that Mn_I converts into Mn_{Ga} by combining with Ga vacancies (V_{Ga}) produced during implantation. We will discuss this below in terms of the thermal stability and diffusion of Mn_I.

$T > 600°$**C:** While the interstitial fraction remains negligible, the substitutional fraction decreases from nearly 100% at 600°C to nearly 50% at 700°C, in both the n^+ and semi-insulating samples. We will discuss this below in terms of long-range diffusion of substitutional Mn.

1. *Interstitial Mn*

The most obvious observation is that the thermal stability of interstitial Mn is independent of the electrical doping of the material. Interpreting this polarity independence requires a closer look at the concentrations of the potentially trapping acceptor and donor defects, which are compiled in Table II. The order of magnitude of the dopant (Zn and Te) concentrations can be estimated from the quoted carrier concentration (before implantation) assuming a 100% activation. After implantation, the Mn_{Ga}/Mn_I fraction contributes with the corresponding acceptor/donor concentration. Note that, although deep centers introduced during implantation are likely to shift the Fermi level towards the middle of the band-gap, thus reducing the number of band carriers, the concentration of *charged* donors (Te_{As} and Mn_I) and acceptors (Zn_{Ga} and Mn_{Ga}) is in principle unaffected, because shallow donors/acceptors remain positively/negatively charged when the Fermi level moves deeper into the bandgap. Since varying the concentration of (potentially) trapping deffects by an order of magnitude (and thus the mean distance between them and the Mn_I defects by almost a factor of 3) produced no measurable change in the thermal stability of Mn_I, these can be ignored in the following modeling of the Mn_I migration.

As mentioned above, the fact that the total $S_{Ga} + T_{As}$ fraction remains constant indicates that Mn_I converts into Mn_{Ga} by combining with Ga vacancies (V_{Ga}) produced during implantation. However, estimating the migration barrier of Mn_I, i.e. the activation energy (E_a) for diffusion, requires that the concentration profiles of both Mn_I and V_{Ga} (before each of the annealing steps) are known. Nevertheless, using the model which we applied to the p^+ case,[12] one can still obtain simple estimates for the maximum and minimum E_a values as follows.

Within an Arrhenius model for the thermally activated migration, the fraction $f(T, \Delta t)$ of Mn remaining on T_{As} sites after an annealing step of duration Δt at a temperature T is given by

$$f(T, \Delta t) = f_0 \exp[-\nu_0 \Delta t / N \exp(-E_a / k_B T)], \qquad (1)$$

where f_0 is the fraction before the annealing step, ν_0 is the attempt frequency, which we take as 10^{12} s^{-1}, *i.e.* of the order of the lattice vibrations, N is the average number of jumps before a Mn_I atom combines with a Ga vacancy and k_B is the Boltzmann constant.[29] Conservative estimates for the minimum and maximum migration energies can be deduced from the two limiting cases for the value of N corresponding to two opposite scenarios before the mobilization of Mn_I: (1) every Mn_I

polarity	dopant	acceptor concentration [at. cm^{-3}]	donor concentration [at. cm^{-3}]	Mn_{Ga} (acceptor) peak concentration [at. cm^{-3}]	Mn_I (donor) peak concentration [at. cm^{-3}]	mean acceptor-acceptor distance [Å]	mean donor-donor distance [Å]
n^+	Te	-	$1.1 - 5\times10^{18}$	3.2×10^{18}	1.6×10^{18}	85	65
s.i.	-	-	-	4.7×10^{18}	2.0×10^{18}	79	54
p^+	Zn	$1.4 - 6\times10^{19}$	-	3.8×10^{18}	1.4×10^{18}	34	90

TABLE II: Estimated donor (Te_{As} and Mn_I) and acceptor (Zn_{Ga} and Mn_{Ga}) concentrations and mean donor-donor and acceptor-acceptor distances. The values corresponding to our previous work on p^+ GaAs [L. M. C. Pereira *et al.*, Appl. Phys. Lett. **98**, 201905 (2011)] are also included.

(in T_{As}) has trapped one mobile V_{Ga} in a neighboring Ga-tetrahedron; (2) Mn_I and V_{Ga} are randomly and independently distributed. Case (1) requires a minimum N of one jump of the Mn atom from T_{As} into the Ga vacancy. Case (2) is rather more complex and an accurate solution requires assumptions to be made about the annealing dynamics of V_{Ga}. Nonetheless, one can estimate a maximum value of N from the following. The root-mean-square (rms) distance traveled by a Mn_I atom after N jumps in a 3-dimensional random walk is given by $R_{rms} = \sqrt{N} \times l$, where l is the distance between two T_{As} sites (4.0 Å). The maximum number of jumps is thus related to the maximum distance traveled by a Mn_I atom before combining with a Ga vacancy, for which a limit can be estimated from our data as follows. Long-range diffusion has a strong effect on the emission patterns due to the exponential dependence of β^- dechanneling on the emitter (^{56}Mn) depth. Diffusion of Mn_I to the surface, *i.e.* over a distance of R_p, would lead to an apparent increase of fitted fractions. Conversely, diffusion of a similar magnitude into the bulk would damp this fraction, resulting in the opposite effect. Since the total $S_{Ga} + T_{As}$ fraction remained constant throughout the annealing sequence, one can take R_p as the maximum distance traveled by the Mn_I atoms in the direction perpendicular to the surface. Statistically, only one third of the jumps result in displacements in that direction. The maximum R_{rms} is hence $3 \times R_p$, corresponding to a maximum N of the order of 20000. With N between 1 and 20000, Eq. (1) yields an activation energy of 1.7–2.3 eV, just as in p^+ GaAs.[12]

The main conclusion from the analysis above is that the high activation energy for Mn_I diffusion in GaAs (1.7–2.3 eV), determined here and in Ref. 12, can not be ascribed to acceptor trapping, and should thus be a characteristic of isolated interstitial Mn (answering question 1 in the Introduction). This does not mean that Mn_I trapping by acceptor defects does not happen in general. In the low concentration regime studied here, it is very likely that trapping does not occur simply because Mn_I defects combine with Ga vacancies before being trapped by substitutional acceptors. For higher Mn concentrations (or more precisely: higher Mn_{Ga} acceptor concentrations) trapping is indeed very likely to occur. We discuss this in more detail below, together with the general implications of this high thermal stability on the strategies to increase T_C in ferromagnetic $Ga_{1-x}Mn_xAs$.

2. Substitutional Mn

The decrease in substitutional fraction from nearly 100% at 600°C to nearly 50% at 700°C indicates Mn diffusion, either to (i) the sample bulk or to (ii) the surface. Electrons emitted from deeper within the sample (i) are subject to stronger dechanneling, which results in a decreased fitted fraction. Electrons emitted from the first few atomic layers at the surface (ii) do not experience channeling effects and thus contribute with an isotropic ("random") pattern, which would also lead to a decreased fitted fraction. In principle, Mn clustering into a phase that is incoherent with the GaAs structure could also explain the decreased substitutional fraction. Clustering is however extremelly unlikely in our samples, given the very small Mn concentrations ($< 0.05\%$). Also material degradation (due to loss of As by annealing in vacuum) could in principle result in enhanced dechanneling and thus a decreased fitted fraction. We have tested this hipothesis by performing ^{73}As:GaAs emission channeling experiments under the same annealing conditions: the ^{73}As substitutional fraction, nearly 100% at 600°C did not decrease upon annealing up to 750°C, which shows that the decrease in substitutional Mn fraction can not be ascribed to sample degradation.

Diffusion of substitutional Mn in GaAs can be modeled by a Frank-Turnbull mechanism: a Mn atom "jumps" from the substitutional site and diffuses through interstitial sites until being trapped by a Ga vacancy (V_{Ga}), thus becoming substitutional (Mn_{Ga}) again. The next "diffusion step" occurs when the atom leaves the vacancy again and finds another one. Considering the V_{Ga} concentration fixed, such a process follows an Arrhenius behavior with the activation energy being the binding energy of Mn to V_{Ga} plus the migration energy of interstitial Mn diffusion, which is in fact the activation energy of Mn_{Ga} becoming interstitial. The Mn_{Ga} fraction measured after an annealing step of duration Δt at a temperature T is thus given by eq. 1, where N is in this case the number of steps until the ^{56}Mn emitter is either too deep to contribute with a measurable channeling effect, or at the surface. Assuming that the concentration of Ga vacancies that survived annealing up to 700°C is residual, only

one diffusion step is required, i.e. $N = 1$. As such, eq. 1 yields $E_a = 2.9$ eV (see Fig. 4), which is in agreement with a recent radio-tracer study on the diffusion of Mn in GaAs,[30] yielding and activation energy of ∼3 eV and higher for a fast and a slow component, respectively.

3. *Comparison to higher Mn concentrations*

When discussing the implications of our results on the strategies for increasing T_C in $Ga_{1-x}Mn_xAs$ (question 2 in the Introduction), one must take into account how the mobility of both interstitial and substitutional Mn may be affected by increasing the Mn concentration from $< 0.05\%$ (this work) up to a few % in ferromagnetic $Ga_{1-x}Mn_xAs$.

Interstitial Mn. Increasing the Mn concentration up to a few % reduces the mean distance between isolated Mn_I atoms and their closest Mn_{Ga} neighbors down to the order of the lattice constant. The migration energy of a Mn_I donor can respond to one such nearby Mn_{Ga} acceptor in two stages, i.e. before and after the Mn_I–Mn_{Ga} nearest-neighbor pair is formed. Before, the positively Mn_I donor is subject to an atractive Coulomb interaction with the negativelly charged Mn_{Ga} acceptor, which in principle *decreases* the energy barrier for migration towards Mn_{Ga}. Once the pair is formed, the same atractive Coulomb potential *increases* the migration energy by an amount which can be regarded as the pair dissociation energy. Such dissociation energies can be as high as 0.8 eV, depending on the structure of the Mn_I–Mn_{Ga} complex, as calculated in Ref. 13. According to the calculations in Ref. 9, the presence of other nearby Mn_{Ga} acceptors reduces somewhat the dissociation energy (as the Coulomb atraction they exert on the Mn_I donor counteracts that within the pair), but the migration energy still remains higher that that of isolated Mn_I, which we determined here to be 1.7–2.3 eV.

Substitutional Mn. In principle, strain and alloying effects resulting from an increasing Mn concentration decrease the migration energy of substitutional Mn, i.e. favor the diffusion towards aggregation and eventual segregation into secondary phases. Indeed, it has been observed in $Ga_{1-x}Mn_xAs$ (∼8% Mn) that part of the substitutional Mn fraction converts to random clusters already at 282°C,[10] i.e well below the 600 – 700 °C interval (determined here) in which susbtitutional Mn becomes mobile in the very dilute regime. Similarly, Mn clustering in $Ga_{1-x}Mn_xAs$ (∼12% Mn) has been suggested to account for the decrease in T_C with increasing annealing temperatures between 160°C and 220°C.[11]

In short, we have determined here that isolated Mn_I in GaAs has a high migration energy (1.7–2.3 eV) and it has been predicted[11,13] that Mn_I–Mn_{Ga} complex formation, which is favored in high Mn concentration $Ga_{1-x}Mn_xAs$, increases it even further. This implies that the annealing temperatures required to induce the out-diffusion of interstitial Mn in $Ga_{1-x}Mn_xAs$ are within the range which is known to induce Mn segregation. This is however in disagreement with the established belief that thermal annealing of $Ga_{1-x}Mn_xAs$ at ∼200°C removes interstitial Mn by inducing its out-diffusion (with an activation energy of 0.7 eV).

Other hints can be found in the literature which indicate that interstitial Mn is *not* removed by low temperature (∼200°C) annealing. Although ion channeling measurements qualitatively detected a decrease of the Mn_I fraction after annealing at 282 °C,[10] they show that at least a significant fraction actually persisted, i.e, almost 100 °C above the temperature at which Mn_I would become mobile if it was the low temperature diffuser. Moreover, using secondary ion-mass spectrometry (SIMS), the out-diffusion of Mn in $Ga_{1-x}Mn_xAs$ was indeed found to be almost negligible below 400°C,[31] with a diffusion coefficient at 200°C that is at least four orders of magnitude smaller than the one derived for the out-diffusion of the donor defect in Ref. 9.

A scenario that would conform to all the observations summarized above is that the defect which out-diffuses at ∼200°C is not interstitial Mn but another compensating defect. In this scenario, Mn_I becomes mobile at slightly higher temperatures and, instead of out-diffusing as generally accepted, it is captured by substitutional Mn, forming complexes which may in fact play the role of seeds for nucleation and segregation of MnAs phases, which takes place at even higher temperatures.[32] In order to complete this scenario, one must identify a defect, other than interstitial Mn, that (i) is created in sufficient abundance during $Ga_{1-x}Mn_xAs$ growth, (ii) compensates substitutional Mn acceptors both electrically and magnetically and (iii) is removed by low temperature (∼200°C) annealing. A detailed discussion is out of the scope of this paper, but for the sake of completeness, we will briefly describe how a defect consisting of non-substitutional (excess) As forming complexes with substitutional Mn fulfills all these three conditions. Low temperature molecular beam epitaxy (LT-MBE) growth of GaAs (∼200°C), as is required for $Ga_{1-x}Mn_xAs$ with high Mn content, produces excess As in the % range[33] [condiction (i)]. Excess non-substitutional As atoms, known to act has deep donors,[34,35] were found to form paramagnetic complexes with Mn_{Ga} in $Ga_{1-x}Mn_xAs$,[36] thus compensating Mn_{Ga} both electrically and magnetically [condition (ii)]. Non-substitutional As in GaAs is known to be removed by thermal annealing in the 200 – 220 °C range,[37] and indeed in Ref. 36, the dissociation of these complexes during 260°C annealing was correlated with the increase in hole concentration and T_C [condition (iii)].

IV. CONCLUSIONS

We have experimentally determined the lattice location of Mn impurities (< 0.05%) in undoped (semi-insulating) and heavily *n*-type doped GaAs, as a funciton of annealing temperature up to ∼700°C. In addition to the majority substituting for Ga, a significant fraction occupies tetrahedral interstitial sites with As nearest neighbors. Similar to our recent results on heavily *p*-type doped GaAs, the interstitial fraction is stable up to 400°C, with an activation energy for diffusion of 1.7–2.3 eV. Substitutional Mn becomes mobile at higher temperatures, ∼700°C, with an activation energy of ∼3 eV.

Since varying the GaAs polarity, and thus the concentration of potentially trapping defects, has no measurable effect on the migration energy of the interstitial fraction, we conclude that the observed high thermal stability is characteristic of isolated interstitial Mn. In $Ga_{1-x}Mn_xAs$ materials with high Mn concentrations, although the electric fields induced by neighboring substitutional Mn acceptors may reduce the migration barrier of interstitial Mn donors, this would in principle favor complex formation, which in turn has previously been predicted to increase the activation energy for out-diffusion of interstitial Mn compared to when the defect is isolated.

Being difficult to reconcile with the general belief that interstitial Mn is the donor defect that out-diffuses at ∼200°C, these findings motivate a careful reassessment of the structural effects of low temperature annealing of $Ga_{1-x}Mn_xAs$. If confirmed, a thermal stability of interstitial Mn above 200°C has major implications on the prospects for increasing T_C in $Ga_{1-x}Mn_xAs$. If interstitial Mn remains in the matrix after low temperature annealing, full activation of the nominal Mn concentration may still be achieved by alternative post-growth processing methods. Since it is believed that a T_C of 300 K can be achieved with $x \approx 0.10$ of purely substitutional Mn, such post-growth processing may potentially allow for the realization of room temperature ferromagnetism in $Ga_{1-x}Mn_xAs$ without further film growth development, as it is currently possible to grow high quality films with $x > 0.10$ (where a fraction is however incorporated interstitially).

Acknowledgments

This work was supported by the Portuguese Foundation for Science and Technology (CERN/FP/109272/2009, CERN/FP/116320/2010, SFRH/BD/35761/2007), the Research Foundation - Flanders, the EURONS project (RII3-CT-2004-506065), the SPIRIT (Support of Public and Industrial Research using Ion Beam Technology) project (contract no. 227012), KULeuven projects GOA/2009/006 and INPAC EF/05/005 and the IUAP P6/42 program.

* e-mail address:linomcp@fc.up.pt

[1] T. Dietl, H. Ohno, F. Matsukura, J. Cibert, and D. Ferrand, Science **287**, 1019 (2000).

[2] K. Sato, P. H. Dederics, and H. Katayama-Yoshida, Europhys. Lett. **61**, 403 (2003).

[3] K. Alberi, K. M. Yu, P. R. Stone, O. D. Dubon, W. Walukiewicz, T. Wojtowicz, X. Liu, and J. K. Furdyna, Phys. Rev. B **78**, 075201 (2008).

[4] T. Dietl, D. D. Awschalom, M. Kaminska, and H. Ohno, *Spintronics*, vol. 82 (Academic Press, 2008).

[5] T. Dietl, Nat. Mater. **9**, 965 (2010).

[6] T. Jungwirth, K. Y. Wang, J. Masek, K. W. Edmonds, J. Konig, J. Sinova, M. Polini, N. A. Goncharuk, A. H. MacDonald, M. Sawicki, et al., Phys. Rev. B **72**, 165204 (2005).

[7] H. Ohno, A. Shen, F. Matsukura, A. Oiwa, A. Endo, S. Katsumoto, and Y. Iye, Appl. Phys. Lett. **69**, 363 (1996).

[8] T. Hayashi, Y. Hashimoto, S. Katsumoto, and Y. Iye, Appl. Phys. Lett. **78**, 1691 (2001).

[9] K. W. Edmonds, P. Boguslawski, K. Y. Wang, R. P. Campion, S. N. Novikov, N. R. S. Farley, B. L. Gallagher, C. T. Foxon, M. Sawicki, T. Dietl, et al., Phys. Rev. Lett. **92**, 037201 (2004).

[10] K. M. Yu, W. Walukiewicz, T. Wojtowicz, I. Kuryliszyn, X. Liu, Y. Sasaki, and J. K. Furdyna, Phys. Rev. B **65**, 201303 (2002).

[11] M. Wang, R. P. Campion, A. W. Rushforth, K. W. Edmonds, C. T. Foxon, and B. L. Gallagher, Appl. Phys. Lett. **93**, 132103 (2008).

[12] L. M. C. Pereira, U. Wahl, S. Decoster, J. G. Correia, M. R. da Silva, A. Vantomme, and J. P. Araújo, Appl. Phys. Lett. **98**, 201905 (2011).

[13] V. I. Baykov, P. A. Korzhavyi, and B. Johansson, Phys. Rev. Lett. **101**, 177204 (2008).

[14] H. Hofsass and G. Lindner, Phys. Rep. **201**, 121 (1991).

[15] U. Wahl, J. G. Correia, S. Cardoso, J. G. Marques, A. Vantomme, G. Langouche, and ISOLDE Collaboration, Nucl. Instrum. Methods Phys. Res. B **136**, 744 (1998).

[16] S. Agostinelli, J. Allison, K. Amako, J. Apostolakis, H. Araujo, P. Arce, M. Asai, D. Axen, S. Banerjee, G. Barrand, et al., Nucl. Instrum. Methods Phys. Res. Sect. A-Accel. Spectrom. Dect. Assoc. Equip. **506**, 250 (2003).

[17] J. Allison, K. Amako, J. Apostolakis, H. Araujo, P. A. Dubois, M. Asai, G. Barrand, R. Capra, S. Chauvie, R. Chytracek, et al., IEEE Trans. Nucl. Sci. **53**, 270 (2006).

[18] H. Hofsass, U. Wahl, and S. G. Jahn, Hyperfine Interact. **84**, 27 (1994).

[19] H. Hofsass, Hyperfine Interact. **97**, 247 (1996).

[20] U. Wahl, Hyperfine Interact. **129**, 349 (2000).

[21] U. Wahl, J. G. Correia, J. P. Araujo, E. Rita, and S. J. C, Appl. Phys. Lett. **90**, 181934 (2007).

[22] L. M. C. Pereira, U. Wahl, S. Decoster, J. G. Correia, L. M. Amorim, M. R. da Silva, , J. P. Araújo, and A. Vantomme (????), (unpublished).

[23] L. M. C. Pereira, U. Wahl, S. Decoster, J. G. Correia,

M. R. da Silva, , J. P. Araújo, and A. Vantomme (????), (unpublished).
[24] R. Bacewicz, A. Twarog, A. Malinowska, T. Wojtowicz, X. Liu, and J. K. Furdyna, J. Phys. Chem. Sol. **66**, 2004 (2005).
[25] V. N. Fedoseyev, K. Batzner, R. Catherall, A. H. M. Evensen, D. ForkelWirth, O. C. Jonsson, E. Kugler, J. Lettry, V. I. Mishin, H. L. Ravn, et al., Nucl. Instrum. Methods Phys. Res. Sect. B-Beam Interact. Mater. Atoms **126**, 88 (1997).
[26] U. Wahl, A. Vantomme, G. Langouche, and ISOLDE collaboration, Nucl. Instrum. Methods Phys. Res. B **148**, 492 (1999).
[27] K. Lawniczak-Jablonska, J. Libera, A. Wolska, M. T. Klepka, R. Jakiela, and J. Sadowski, Rad. Phys. Chem. **78**, S80 (2009).
[28] A. Wolska, K. Lawniczak-Jablonska, M. T. Klepka, R. Jakiela, J. Sadowski, I. N. Demchenko, E. Holub-Krappe, A. Persson, and D. Arvanitis, Act. Phys. Pol. **114**, 357 (2008).
[29] U. Wahl, J. G. Correia, E. Rita, J. P. Araujo, J. C. Soares, and ISOLDE Collaboaration, Nucl. Instrum. Methods Phys. Res. B **253**, 167 (2006).
[30] O. Koskelo, J. Raisanen, F. Tuomisto, J. Sadowski, and ISOLDE Collaboration, Sem. Sci. Tech. **24**, 045011 (2009).
[31] R. E. Goacher, S. Hegde, H. Luo, and J. A. Gardella, J. Appl. Phys. **106**, 044302 (2009).
[32] A. Kwiatkowski, D. Wasik, M. Kaminska, R. Bozek, J. Szczytko, A. Twardowski, J. Borysiuk, J. Sadowski, and J. Gosk, J. Appl. Phys. **101**, 113912 (2007).
[33] Kin Man Yu, M. Kaminska, and Z. Liliental-Weber, J. Appl. Phys. **72**, 2850 (1992).
[34] S. Ohagan and M. Missous, J. Appl. Phys. **75**, 7835 (1994).
[35] H. Shimizu, T. Hayashi, T. Nishinaga, and M. Tanaka, Appl. Phys. Lett. **74**, 398 (1999).
[36] Y. Ishiwata, M. Watanabe, R. Eguchi, T. Takeuchi, Y. Harada, A. Chainani, S. Shin, T. Hayashi, Y. Hashimoto, S. Katsumoto, et al., Phys. Rev. B **65**, 233201 (2002).
[37] J. C. Bourgoin, H. J. Vonbardeleben, and D. Stievenard, J. Appl. Phys. **64**, R65 (1988).